PERGAMON

Significance of dimensionality and dynamical screening on hot carrier relaxation in bulk GaAs and quantum wells

H.C. Lee[a,*], K.W. Sun[b], C.P. Lee[a]

[a]*Department of Electronic Engineering and Institute of Electronics, National Chiao Tung University, 1001 Ta Hsueh Road, Hsinchu, Taiwan, ROC*
[b]*Department of Physics, National Dong Hwa University, Hualien, Taiwan, ROC*

Abstract

We have found theoretically that the reduced dimensionality from bulk GaAs to quantum wells has a strong effect on hot carrier relaxations at highly excited carrier densities. The distinct density of state and the dynamical screening cause hot carriers in quantum wells to relax significantly slower than in the bulk when the carrier density is above a critical value of 2×10^{18} cm^{-3}. With the random phase approximation, the dynamical screening in quantum wells appears to be much stronger than that in the bulk and as important as the hot phonon effect at high carrier densities. We also found that the dependence of the average energy-loss rates on the well width in quantum wells becomes more appreciable when Al compositions are high.
© 2003 Elsevier Ltd. All rights reserved.

1. Introduction

Although hot carrier relaxations in a bulk GaAs and quantum wells have been studied experimentally [1–11] and theoretically [12–14] for more than one decade, the dependence of the dynamical screening in hot carrier relaxations on the sample's dimensionality is still not well understood. The screening behavior caught less attention on hot carrier relaxations in GaAs probably attributes that the hot phonon effect was primarily considered to be responsible for the great drop of energy-loss rates via Fröhlich interaction [2,5,11], and hot carrier relaxations seem not to depend on the dimensionality experimentally [4–6]. However, the deduction could not hold on the overall carrier densities. Because more recent experimental results indicated that there is a clear difference in energy-loss rates between a bulk GaAs and quantum wells when the carrier

density is above a certain critical value [7–9]. Though the critical carrier densities determined in those experiments are not consistent, the results imply that the dimensionality and the dynamical screening may have a significant effect on hot carrier relaxations in a bulk GaAs and quantum wells.

To theoretically study the difference of hot carrier relaxations between the two different dimensional systems, it is important to consider the optical phonon modes in a quantum well. Many improved models were developed to give a better description for atomic vibrations and the interaction Hamiltonians with electrons in the quasi two-dimensional (2D) structure [15–26]. In our calculations, we use the dielectric continuum model (DCM) [15–17,20] because the model has provided a good agreement with many earlier experimental results [27–33]. Although the interaction Hamiltonians of phonon modes in a quantum well are strongly dependent on the well width, many experimental results [4–6] demonstrated the less well-width dependence of hot carrier relaxations except for the few reports that show the contrary results [34,35]. This

* Corresponding author. Tel.: +886-3571-2121-54240; fax: +886-357-243-61.

E-mail address: u8711819@cc.nctu.edu.tw (H.C. Lee).

discrepancy also stimulates us to study the structural dependence of energy-loss rates in a quantum well.

In this report, the significance of the dimensionality and the dynamical screening on hot carrier relaxations in a bulk GaAs and quantum wells is investigated. The distinct dimensionality and the dynamical screening indeed cause that hot carriers in quantum wells relax significantly slower than that in a bulk GaAs above the critical carrier density of $2 \times 10^{18} \text{ cm}^{-3}$. We attribute this to the smaller density of state in quantum wells and the strong 2D dynamical screening. The dynamical screening in quantum wells appears to be much stronger than that in the bulk and considerable as compared to the hot phonon effect. The critical carrier density determined in our studied is in very good agreement with the earlier experiments of Pelouch et al. [7]. We also found that the average energy-loss rate (AELR) in quantum wells depends on the well width more appreciably when Al compositions are high.

2. Theory

The AELR is calculated in order to compare the difference of hot carrier relaxations between the two different dimensional systems. In this section, we describe the derivations of the AELR in a bulk GaAs and a quantum well, where the net phonon generation rate and the treatments of hot phonon effect and the dynamical screening are included. The dynamical screening is dealt with the random phase approximation (RPA) [36]. Exact dimensional treatments are handled on the AELR's derivations and the dynamical screenings. In our calculations, the electron–phonon scattering is through Fröhlich interaction and only intrasubband scattering is considered in the calculation of the AELR in quantum wells. The hole–phonon interaction is neglected. The plasmon–phonon coupling (PPC) is not considered here because the significant enhancement of energy-loss rates [37,38] induced by the PPC does not appear above the critical carrier density of $2 \times 10^{18} \text{ cm}^{-3}$.

The AELR is determined by the net phonon generation rate and the phonon energy. The net phonon generation rate represents the subtracting difference between phonon's generation rates and absorption rates. In a bulk GaAs, the three-dimensional (3D) net phonon generation rate is given by [39]

$$\frac{\partial N_{\vec{q}}}{\partial t} = \frac{m_e^2 k_B T_C V}{\pi \hbar^5 q} |M_{\vec{q}}|^2 [N_{\vec{q}}(T_C) - N_{\vec{q}}] \int_{\varepsilon_{\min}}^{\infty}$$
$$\times \left[f(\varepsilon) - f\left(\varepsilon + \frac{\hbar \omega_{\vec{q}}}{k_B T_C}\right) \right] \mathrm{d}\varepsilon \quad (1)$$

where q and $\omega_{\vec{q}}$ denote phonon's wave vector and phonon's energy, respectively. $f(\varepsilon)$ is the electron's distribution. With the thermalized assumption for carriers, Fermi–Dirac distribution is used where T_C is the carrier temperature. $N_{\vec{q}}$

represents phonon population. m_e, k_B, and V have their usual meanings. The quantity $N_{\vec{q}}(T_C)$ can be written as [39]

$$N_{\vec{q}}(T_C) = \frac{1}{\exp\left(\dfrac{\hbar \omega_{\vec{q}}}{k_B T_C}\right) - 1} \quad (2)$$

where ε, a dimensionless quantity, represents the normalized energy (energy divided by thermal energy $k_B T_C$). $\varepsilon_{\min}$ is the minimum normalized energy required for an electron to kick out a phonon of wave vector $\vec{q}$. It is given by [39]

$$\varepsilon_{\min} = \frac{m_e}{2\hbar^2 q^2 k_B T_C} \left| \frac{\hbar^2 q^2}{2 m_e} - \hbar \omega_{\vec{q}} \right|^2 \quad (3)$$

$|M_{\vec{q}}|^2$, Fröhlich interaction strength, is given by [39]

$$|M_{\vec{q}}|^2 = \frac{e^2 \hbar \omega_{\vec{q}}}{2 V q^2 \varepsilon_0} \left(\frac{1}{\kappa_\infty} - \frac{1}{\kappa_S} \right) \quad (4)$$

where κ_∞ and κ_S are high frequency and static relative dielectric constants, respectively.

In a quantum well, based on the DCM [15–17,20], the confined (C), the symmetric plus interface (S +), symmetric minus (S −) interface, and the half-space (HS) phonon modes are considered in our calculations. Antisymmetric interface modes are excluded due to the selection rule for the intrasubband scattering. The dispersion relations for the S + and the S − interface modes are shown in our earlier report [40]. The noun 'half-space' in double heterojunctions originates from the report of Mori and Ando [20], where the same name as the case of a single heterojunction is used. The 2D net phonon generation rate can be written as

$$\frac{\partial N_{\vec{q}_\parallel}^{(C,S\pm,HS)}}{\partial t} = \frac{\sqrt{2 m_n^3 k_B T_C} A}{\pi \hbar^4 q_\parallel} |M_{\vec{q}_\parallel}^{(C,S\pm,HS)}|^2 [N_{\vec{q}_\parallel}^{(C,S\pm,HS)}(T_C)$$
$$- N_{\vec{q}_\parallel}^{(C,S\pm,HS)}] \int_{\varepsilon_{\min}}^{\infty} \frac{1}{\sqrt{\varepsilon}}$$
$$\times \left[f(\varepsilon + \varepsilon_1) - f\left(\varepsilon + \varepsilon_1 + \frac{\hbar \omega_{\vec{q}_\parallel}^{(C,S\pm,HS)}}{k_B T_C}\right) \right] \mathrm{d}\varepsilon$$
$$(5)$$

where $\vec{q}_\parallel$ and $\omega_{\vec{q}_\parallel}^{(C,S\pm,HS)}$ denote the in-plane phonon wave vector and the phonon energies of various modes. m_n is the nth layer effective mass while 1 represents GaAs and 2 represents AlGaAs layers. A denotes the area. ε_1 is the normalized ground state energy to the thermal energy. $|M_{\vec{q}_\parallel}^{(C,S\pm,HS)}|^2$ represents the electron–phonon interaction strength of various modes shown in Table 1. The used Hamiltonians are taken from the report of Mori and Ando [20].

The quantity of $N_{\vec{q}(\vec{q}_\parallel)}^{(C,S\pm,HS)}$ is to be determined. When the hot phonon effect is excluded, the phonon population satisfies the Bose–Einstein relation with a lattice temperature T_L. In general, the hot phonon effect plays an important role in hot carrier relaxations. The phonon dynamics can be

Table 1
The electron–optical-phonon interaction strengths in a quantum well structure

Optical-phonon mode	Interaction strength
Symmetric $\pm$ interface modes[a]	$|M_{\vec{q}_\parallel}^{S\pm}|^2 = \dfrac{e^2\hbar\omega_{\vec{q}_\parallel}^{S\pm}}{4Aq\epsilon_0}[\beta_1^{-1}(\omega_{\vec{q}_\parallel}^{S\pm})\tanh\left(\dfrac{1}{2}q_{//}L\right) + \beta_2^{-1}(\omega_{\vec{q}_{//}}^{S\pm})]^{-1}|G_{S\pm}^n|^2,$ where n $= \begin{cases} 1 : \text{the wellregion} \\ 2 : \text{barrier regions} \end{cases}$
Confined mode[a,b]	$|M_{\vec{q}_\parallel}^C|^2 = \dfrac{e^2\hbar\omega_{\vec{q}_\parallel}^C}{V\varepsilon_0}\left(\dfrac{1}{\kappa_{\infty 1}} - \dfrac{1}{\kappa_{S1}}\right)\dfrac{1}{q_\parallel^2 + (p\pi/L)^2}|G_C^p|^2$
Half-space mode[a,b,c]	$|M_{\vec{q}_\parallel}^{HS}|^2 = \displaystyle\int_0^\infty \dfrac{e^2\hbar\omega_{\vec{q}_\parallel}^{HS}}{2\pi A\varepsilon_0}\left(\dfrac{1}{\kappa_{\infty 2}} - \dfrac{1}{\kappa_{S2}}\right)\dfrac{1}{q_\parallel^2 + q_z^2}|G_{HS}|^2 dq_z$

[a] $G_{S\pm}^n$ is $\langle \varphi_1|\phi_{S\pm}|\varphi_1\rangle$, where φ_1 is the electron's ground state and $\phi_{S\pm}$ is potential for interface modes, and the factors G_C^p, G_{HS} are the overlap integral for the pth confined mode and the half-space mode, respectively. Their expressions are given in the Ref. [40].

[b] $\kappa_{\infty n}$, κ_{Sn} are nth high frequency and static relative dielectric constants.

[c] q_z is the phonon wave vector paralleled to the crystal's growth direction.

governed by the phonon Boltzmann equation. At the steady state, the phonon's population can be given by the following equation with using Eq. (1) for bulk (Eq. (5) for quantum wells) [39].

$$\frac{\partial N_{\vec{q}(\vec{q}_\parallel)}^{(C,S\pm,HS)}}{\partial t} = \frac{N_{\vec{q}(\vec{q}_\parallel)}^{(C,S\pm,HS)} - N_{\vec{q}(\vec{q}_\parallel)}^{(C,S\pm,HS)}(T_L)}{\tau_{ph}} \qquad (6)$$

where τ_{ph} is the phonon life time.

The dynamical screening on hot carrier relaxations is handled with the electronic dielectric function. Based on the RPA, the dielectric function is given by [36]

$$\varepsilon_{el}(\vec{q},\omega) = 1 + 2V_{\vec{q}}\sum_{\vec{k}}\frac{f(E(\vec{k}+\vec{q})) - f(E(\vec{k}))}{\hbar\omega + E(\vec{k}+\vec{q}) - E(\vec{k}) + i\gamma} \qquad (7)$$

where $V_{\vec{q}}$ is the Fourier transform of the Coulomb interaction. The damping coefficient γ ranges from 0.2 to 0.3 times of the plasma frequency [41].

According to the result from the derivation of Haug and Koch [42] with the RPA, the effective screened electron–phonon interaction strength $|M_{\vec{q}}^{eff}|^2$ can be expressed as

$$|M_{\vec{q}}^{eff}|^2 = \left|\frac{M_{\vec{q}}}{\varepsilon_{el}(\vec{q},\omega)}\right|^2 \qquad (8)$$

The 3D and 2D zero-temperature dielectric functions are,

respectively, given by [43]

$$\varepsilon_{el}^{3D}(\vec{q},\omega_{\vec{q}}) = 1 + \frac{3n_{3D}e^2}{4\varepsilon_0\kappa_\infty q^2 E_F}$$

$$\times\left\{1 + \frac{k_F}{2q}\left[1 - \left(\frac{\omega_{\vec{q}}+i\gamma}{qv_F} + \frac{q}{2k_F}\right)^2\right]\right.$$

$$\times\ln\left|\frac{\frac{\omega_{\vec{q}}+i\gamma}{qv_F} + \frac{q}{2k_F} + 1}{\frac{\omega_{\vec{q}}+i\gamma}{qv_F} + \frac{q}{2k_F} - 1}\right| - \left[1 - \left(\frac{\omega_{\vec{q}}+i\gamma}{qv_F} - \frac{q}{2k_F}\right)^2\right]$$

$$\left.\times\ln\left|\frac{\frac{\omega_{\vec{q}}+i\gamma}{qv_F} - \frac{q}{2k_F} + 1}{\frac{\omega_{\vec{q}}+i\gamma}{qv_F} - \frac{q}{2k_F} - 1}\right|\right\} \qquad (9)$$

$$\varepsilon_{el}^{2D}(\vec{q}_\parallel,\omega_{\vec{q}_\parallel}^{(C,S\pm,HS)}) = 1 + \frac{n_{2D}e^2}{2\varepsilon_0\kappa_{\infty n}q_\parallel E_F}$$

$$\times\left\{1 - \frac{k_F}{q_\parallel}\left\{\left[\left(\frac{\omega_{\vec{q}_\parallel}^{(C,S\pm,HS)}+i\gamma}{q_\parallel v_F} + \frac{q_\parallel}{2k_F}\right)^2 - 1\right]^{1/2}\right.\right.$$

$$\left.\left. - \left[\left(\frac{\omega_{\vec{q}_\parallel}^{(C,S\pm,HS)}+i\gamma}{q_\parallel v_F} - \frac{q_\parallel}{2k_F}\right)^2 - 1\right]^{1/2}\right\}\right\} \qquad (10)$$

where n_{3D} and n_{2D} denote the volume carrier density and the sheet density. E_F, k_F, and v_F represent Fermi energy, Fermi wave vector, and Fermi velocity, respectively.

Finally, the 3D and 2D AELRs can be obtained by using the definitions shown below

$$(\text{AELR})_{3D} = \frac{1}{n_{3D}V}\sum_{\vec{q}}\hbar\omega_{\vec{q}}\frac{\partial N_{\vec{q}}}{\partial t} \qquad (11)$$

$$(AELR)_{2D} = \frac{1}{n_{2D}A} \sum_{C,S\pm,HS} \sum_{\vec{q}_\parallel, q_z} \hbar\omega_{\vec{q}_\parallel}^{(C,S\pm,HS)} \frac{\partial N_{\vec{q}_\parallel}^{(C,S\pm,HS)}}{\partial t} \quad (12)$$

where q_z is defined in the caption of Table 1.

3. Results and discussion

The material's parameters and the used assumptions are referred [40,44–46]. Our calculations of the reduced dimensionality on hot carrier relaxations are performed on a bulk GaAs and a 10 nm-width single GaAs/Al$_{0.24}$Ga$_{0.76}$As quantum well, where the band-offset ratio of $\Delta E_C : \Delta E_V = 65 : 35$ is used [44]. The average phonon energy is approximated in AlGaAs layers to simplify the two-mode behaviors of the GaAs-like and the AlAs-like phonons [40]. The material's parameters are quoted from Adachi's report [45]. The electron's distribution function is assumed to satisfy with Fermi–Dirac relation. We use 300 K as the electron's temperature except the section reported the structural dependence in quantum wells, where 600 K is taken. An initial lattice temperature is chosen to be 15 K. We quote 7 ps to be the phonon life times in both bulk GaAs and quantum wells [46]. Only first-order mode [20] of confined phonons is considered in our calculation because of the very less contribution to the AELR from higher-order modes. In general, the AELRs in quantum wells are summed over S ± interface and the confined modes.
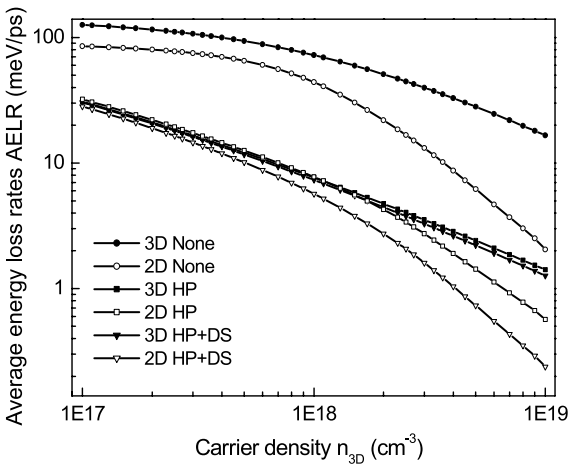
In Fig. 1 we show the dependence of the AELR on the

carrier density in a bulk GaAs and quantum wells where the sheet carrier densities are transferred by n_{2D}/L. To study the influence of the dimensionality and the dynamical screening on hot carrier relaxations, three different conditions are considered and the corresponding curves are plotted in the figure where they are in the absence of the hot phonon effect and dynamical screening (denoted by None in the plot), in the presence of the hot phonon effect (denoted by HP), and in the presence of the hot phonon effect and dynamical screening (denoted by HP + DS). For the first case, the AELRs in the bulk are shown to be higher than that in quantum wells. Above the carrier density of 10^{18} cm^{-3}, the faster decrease in the AELRs in quantum wells than the bulk is found. Because the energy-loss rate in materials is equal to the product of the AELR and the carrier density, this implies that there is a considerable difference in the energy-loss rate between a bulk GaAs and quantum wells as the carrier density is increased. In the absence of hot phonon effect and the dynamical screening, the rapid deviation of the AELRs is only attributed to their different density of state. Due to the smaller density of state, hot carriers in quantum wells are shown to relax considerably slower than that in the bulk above the critical carrier density. With the hot phonon effect, although the AELRs greatly drop in both sample's structures, the rapid deviation of the AELR between a bulk GaAs and quantum wells still appears while the critical carrier density is shifted to the higher one (toward 2×10^{18} cm^{-3}).

In Fig. 2, we show the difference $|AELR_{HP}^{3D} - AELR_{HP}^{2D}|$ on the left axis and the ratio $|AELR_{HP}^{3D} - AELR_{HP}^{2D}|/AELR_{HP}^{2D}$ on the right, where the lower and upper symbols of the AELR represent the considered effect and dimensions, respectively. Below the carrier density of 10^{18} cm^{-3}, slightly higher 2D AELRs are demonstrated and this is

Fig. 1. The dependence of the AELR with different conditions on the carrier density for a bulk GaAs and a 10 nm GaAs/Al$_{0.24}$Ga$_{0.76}$-As quantum well. The confined and the S ± interface modes were considered in the AELR's calculation of a quantum well. The carrier temperature of 300 K and the initial lattice temperature of 15 K were used. The symbols 'None,' 'HP,', and 'HP + DS,' respectively, denote the AELRs in the absence of the hot phonon effect and the dynamical screening, in the presence of the hot phonon effect, and in the presence of the hot phonon effect and the dynamical screening.
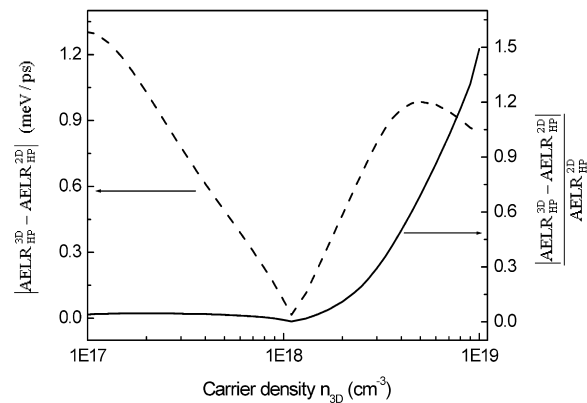

Fig. 2. The left axis of the figure shows the absolute difference of the AELR with the hot phonon effect between a bulk GaAs and a 10 nm GaAs/Al$_{0.24}$Ga$_{0.76}$As quantum well while the right axis shows the percentage change of $|AELR_{HP}^{3D} - AELR_{HP}^{2D}|$ per $AELR_{HP}^{2D}$ as a function of the carrier density. The AELR of the quantum well was obtained by summing the confined and the S ± interface modes. The carrier temperature of 300 K and the initial lattice temperature of 15 K were used.

because the hot phonon effect in quantum wells is weaker than that in the bulk. But, above the carrier density, the effect of the smaller density of state in quantum wells overcomes the hot phonon effect so that 2D AELRs recover to be lower than the 3D case, and the threshold curve clearly shows the significant effect of the distinct density of state on hot carrier relaxations between a bulk GaAs to quantum wells.

In our investigation, the 2D dynamical screening is also found to be an important role on hot carrier relaxations at a high carrier density. Due to the great difference of the dynamical screening between the two different dimensions, the calculated results with the HP + DS in Fig. 1 shows the more rapid deviation of AELRs between the two sample's structures. In order to compare the screening strength between a bulk GaAs and quantum wells, we plot Fig. 3, where the right and left axes, respectively, show reduction factors due to the dynamical screening and the hot phonon effect. The symbols were mentioned earlier. The dynamical screening in quantum wells is shown to be much stronger than that in the bulk and more quickly increased when the carrier density is above 10^{18} cm^{-3}. The quicker increase for the 2D dynamical screening is the consequence of the chemical potential in quantum wells, which is raised faster than that in the bulk as the carrier density is increased. The 2D dynamical screening is also shown to be as important as the hot phonon effect at a high carrier density. To our best knowledge, the earlier investigations [2,4,5] usually omit the effect of the dynamical screening on hot carrier relaxations. In a short summary, because of the fewer density of state and the strong 2D dynamical screening, hot carriers in quantum wells relax significantly slower than that in the bulk at a carrier density above the critical value of 2×10^{18} cm^{-3}. The threshold behavior and the critical carrier density are in very good agreement with the earlier

experimental results [5,7] of Leo [5], Pelouch [7], and their co-researchers.

Next, we interpret the calculated results for the well-width dependence of hot carrier relaxations in quantum wells. The sheet density of 5×10^{11} cm^{-2} is fixed for all calculated results with different structural parameters. Firstly, we show the dependence of the AELR on the well width for various phonon modes in Fig. 4(a), where the S +, S −, the confined, and the half-space modes are considered. The AELRs for the confined mode always increases until to the well width of 10 nm. This is the consequence of the electrons better confined in the wider well and the decreased phonon wave vector parallel to the crystal's growth direction. For the S + interface modes, because the electron's spatial distribution departs from the double interfaces and the decreased Hamiltonian, the AELRs are shown to quickly decrease with the increased well widths. The S − interface and the half-space modes are less noticeable because of the flatter dependence and much smaller AELR as compared to the other modes. In Fig. 4(b), we show the AELRs as functions of the well width and the Al composition by summing over all phonon modes. The opposite dependence on the well width between the confined and the S + interface modes compensates with each other and brings the protruding well-width dependence for various Al compositions. The protruding behavior was also ever found in the earlier experiment of Ryan and Tatham [35]. As the Al composition is increased, the well-width dependence of the AELR becomes more appreciable and the maximum AELR moves toward the shorter well width. The reason is the increasingly stronger effect of the S + interface phonon mode on the hot carrier relaxations with the increased Al composition. The slightly roughness in AELR's curves is the consequence of the numerical inaccuracy from the 2D net phonon generation rate where the finite spike at a given in-plane phonon wave vector is shown in the inset of Fig. 4(b).

4. Conclusions

In conclusion, we theoretically clarify the discrepancies of the earlier experimental results on hot carrier relaxations in bulk GaAs and quantum wells. In contrast to the results in a bulk GaAs, both the dimensionality and the dynamical screening have a significant effect on hot carrier relaxations in quantum wells. The smaller density of state in quantum wells and the strong 2D dynamical screening cause hot carriers in quantum wells to relax significantly slower than that in a bulk GaAs when the carrier density is above 2×10^{18} cm^{-3}. The influence of the 2D dynamical screening on hot carrier relaxations is considerable and is as important as the hot phonon effect when the carrier density is high. As the Al composition is increased, the AELR in quantum wells has a more appreciable dependence on the well width.
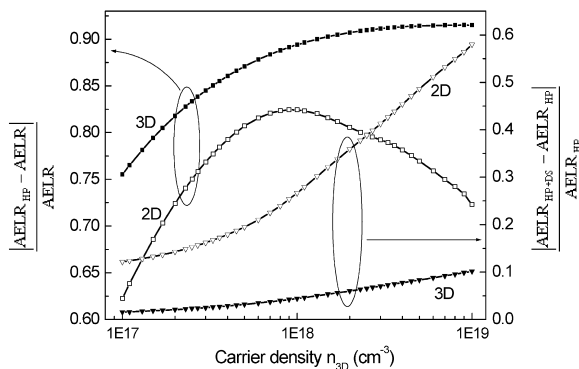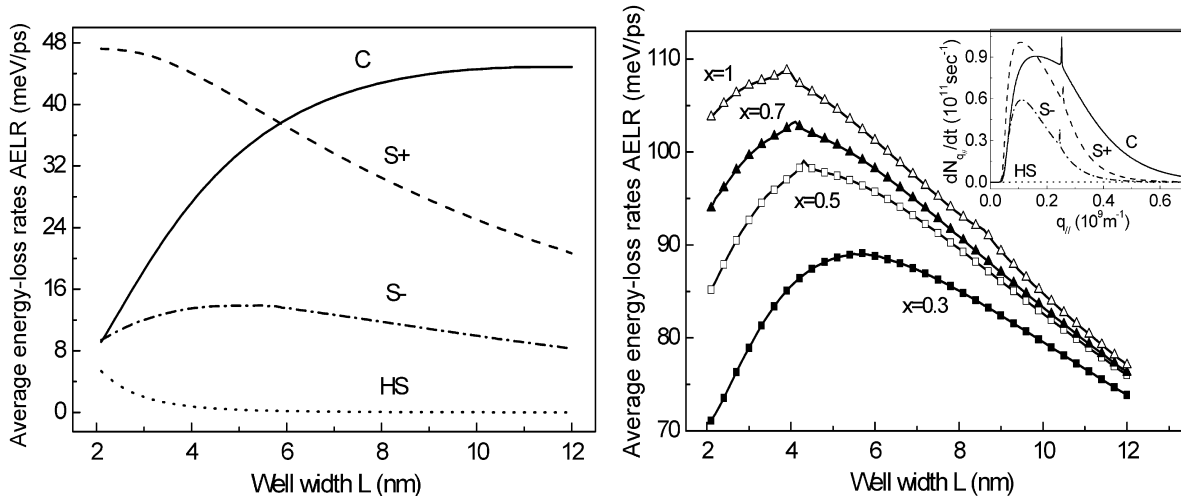

Fig. 3. The plot shows the influence of the hot phonon effect (the left axis) and of the dynamical screening (the right axis) on hot carrier relaxations as a function of carrier density for the bulk GaAs and a 10 nm GaAs/Al$_{0.24}$Ga$_{0.76}$As quantum well. The AELR of a quantum well was obtained by summing the confined and the S ± interface modes. The carrier temperature of 300 K and the initial lattice temperature of 15 K were used.

Fig. 4. (a) The plot shows the AELR with the hot phonon effect for the confined, S $\pm$ interface, and the half-space modes as a function of the well width in a GaAs/Al$_{0.3}$Ga$_{0.7}$As quantum well. The carrier temperature of 600 K, the initial lattice temperature of 15 K, and the carrier density of 5×10^{11} cm^{-2} were used. (b) The dependence of the AELR with the hot phonon effect on the well width in GaAs/Al$_x$Ga$_{1-x}$As quantum wells for Al compositions $x = 0.3$, 0.5, 0.7, and 1. The AELR of the quantum well was obtained by summing the confined, the S $\pm$ interface modes, and the half-space mode. The carrier temperature of 600 K, the initial lattice temperature of 15 K, and the carrier density of 5×10^{11} cm^{-2} were used. The inset plot shows the net phonon generation rates with the hot phonon effect in a 10 nm GaAs/Al$_{0.3}$Ga$_{0.7}$As quantum well as a function of the in-plane phonon wave vector for the confined, the S $\pm$ interface, and the half-space modes.

References

[1] J.F. Ryan, et al., Phys. Rev. Lett. 53 (1984) 1841.
[2] J. Shah, et al., Phys. Rev. Lett. 54 (1985) 2045.
[3] C.H. Yang, et al., Phys. Rev. Lett. 55 (1985) 2359.
[4] H.-J. Polland, et al., Phys. Rev. B 35 (1987) 8273.
[5] K. Leo, et al., Phys. Rev. B 37 (1987) 7121.
[6] C.V. Shank, et al., Solid State Commun. 47 (1983) 981.
[7] W.S. Pelouch, et al., Phys. Rev. B 45 (1992) 1450.
[8] Y. Rosenwaks, et al., Phys. Rev. B 48 (1993) 14675.
[9] Z.Y. Xu, et al., Appl. Phys. Lett. 44 (1984) 692.
[10] K. Kash, et al., Phys. Rev. B 33 (1986) 8762.
[11] H. Lobentanzer, et al., Phys. Rev. B 39 (1989) 5234.
[12] J.F. Young, et al., Phys. Rev. B 47 (1993) 6316.
[13] J.H. Collet, Phys. Rev. B 39 (1989) 7659.
[14] E.J. Yoffa, Phys. Rev. B 23 (1981) 1909.
[15] R.G. Ulbrich, Phys. Rev. B 8 (1973) 5719.
[16] R. Fuchs, et al., Phys. Rev. 140 (1965) A2076.
[17] J.J. Licari, et al., Phys. Rev. B 15 (1977) 2254.
[18] R. Lassnig, Phys. Rev. B 30 (1984) 7132.
[19] K. Huang, et al., Phys. Rev. 38 (1988) 13377.
[20] N. Mori, et al., Phys. Rev. B 40 (1989) 6175.
[21] R. Chen, et al., Phys. Rev. B 41 (1990) 1435.
[22] G.Q. Hai, et al., Phys. Rev. B 48 (1993) 4666.
[23] M.P. Chamberlain, et al., Phys. Rev. B 48 (1993) 14356.

[24] H. Rücker, et al., Phys. Rev. B 45 (1992) 6747.
     H. Rücker, et al., 44 (1991) 3463.
[25] B.K. Ridley, Phys. Rev. B 47(1993) 4592.
     B.K. Ridley, Phys. Rev. B 39 (1989) 5282.
[26] V.N. Stavrou, et al., Phys. Rev. B 63 (2001) 205304–205311.
[27] A.K. Sood, et al., Phys. Rev. Lett. 54 (1985) 2111.
[28] A.K. Sood, et al., Phys. Rev. Lett. 54 (1985) 2115.
[29] J.K. Jain, et al., Phys. Rev. Lett. 62 (1989) 2305.
[30] K.T. Tsen, et al., Phys. Rev. Lett. 67 (1991) 2557.
[31] A.J. Shields, et al., Phys. Rev. Lett. 72 (1994) 412. A.J. Shields, et al., Phys. Rev. B 51 (1994) 17728
[32] A.K. Arora, et al., Phys. Rev. B 36 (1987) 6142.
[33] V.F. Sapega, et al., Phys. Rev. B 52 (1995) 14144.
[34] M. Tatham, et al., Solid State Electron. 31 (1988) 459.
[35] J.F. Ryan, et al., Solid State Electron. 32 (1989) 1429.
[36] G. Mahan, Many Particle Physics, Plenum, New York, 2000.
[37] S.D. Sarma, et al., Phys. Rev. B 37 (1988) 6290.
[38] J. Shah, Solid State Electron. 21 (1978) 43.
[39] J.T. Devreese, et al., The Physics of the Two-Dimensional Electron Gas, Plenum, New York, 1987, pp. 183–225.
[40] H.C. Lee, et al., J. Appl. Phys. 92 (2002) 268.
[41] T. Thoai, et al., Phys. Status Solidi B 98 (1980) 581.
[42] H. Haug, et al., Quantum Theory of Optical and Electronic Properties of Semiconductors, World Scientific, Singapore, 1994, pp. 142–144.
[43] J. Shah, Hot Carriers in Semiconductor Nanostructures: Physics and Applications, Boston, Academic, 1992, p. 61.
[44] C.G.V. de Walle, Phys. Rev. B 39 (1989) 1871.
[45] S. Adachi, J. Appl. Phys. 58 (1985) R1.
[46] J.F. Ryan, et al., Proc. SPIE 942 (1988) 256.